Published in final edited form as:
J Immunol. 2010 August 1; 185(3): 1822–1835. doi:10.4049/jimmunol.0903398.

sRAGE Induces Human Monocyte Survival and Differentiation

Yijie Wang[*,1], **Hongmei Wang**[*,1], **Melissa G. Piper**[*,1], **Sara McMaken**[*], **Xiaokui Mo**[*], **Judy Opalek**[*], **Ann Marie Schmidt**[†], and **Clay B. Marsh**[*]

[*]Division of Pulmonary, Allergy, Critical Care, and Sleep Medicine, Department of Internal Medicine, Dorothy M. Davis Heart and Lung Research Institute, The Ohio State University, Columbus, OH 43210

[†]Department of Surgery, Columbia University Medical Center, New York, NY 10032

Abstract

The receptor for advanced glycation end products (RAGE) is produced either as a transmembrane or soluble form (sRAGE). Substantial evidence supports a role for RAGE and its ligands in disease. sRAGE is reported to be a competitive, negative regulator of membrane RAGE activation, inhibiting ligand binding. However, some reports indicate that sRAGE is associated with inflammatory disease. We sought to define the biological function of sRAGE on inflammatory cell recruitment, survival, and differentiation in vivo and in vitro. To test the in vivo impact of sRAGE, the recombinant protein was intratracheally administered to mice, which demonstrated monocyte- and neutrophil-mediated lung inflammation. We also observed that sRAGE induced human monocyte and neutrophil migration in vitro. Human monocytes treated with sRAGE produced proinflammatory cytokines and chemokines. Our data demonstrated that sRAGE directly bound human monocytes and monocyte-derived macrophages. Binding of sRAGE to monocytes promoted their survival and differentiation to macrophages. Furthermore, sRAGE binding to cells increased during maturation, which was similar in freshly isolated mouse monocytes compared with mature tissue macrophages. Because sRAGE activated cell survival and differentiation, we examined intracellular pathways that were activated by sRAGE. In primary human monocytes and macrophages, sRAGE treatment activated Akt, Erk, and NF-κB, and their activation appeared to be critical for cell survival and differentiation. Our data suggest a novel role for sRAGE in monocyte- and neutrophil-mediated inflammation and mononuclear phagocyte survival and differentiation.

Monocytes are derived from bone marrow precursors and circulate in the blood for 24–48 h. In the absence of growth factors, monocytes die of apoptosis (1). In response to growth factors, tissue injury, or pathogen signals, monocytes can differentiate into tissue macrophages, including liver Kupffer cells, lung alveolar macrophages, brain microglial cells, peritoneal macrophages, bone osteoclasts, and breast mammary macrophages (2, 3). We and others found that PI3K/Akt and Erk activation is important in monocyte survival and macrophage development (2, 4, 5).

Address correspondence and reprint requests to Clay B. Marsh, Division of Pulmonary, Allergy, Critical Care, and Sleep Medicine, Department of Internal Medicine, The Ohio State University, 260 Meiling Hall, 370 West 9th Avenue, Columbus, OH 43210. clay.marsh@osumc.edu.

[1]Y.W., H.W., and M.G.P. contributed equally to this work.

The online version of this article contains supplemental material.

Disclosures

The authors have no financial conflicts of interest.

Monocytes and macrophages express the transmembrane receptor for advanced glycation end products (RAGE) as well as a soluble form (sRAGE). This receptor is a multiligand transmembrane receptor belonging to the Ig super family (6). RAGE was originally identified as receptor for advanced glycation end products (AGE), products of nonenzymatic glycation and oxidation (7). Recent reports clarify that RAGE is a pattern-recognition receptor that binds a variety of ligands, including members of the S100/calgranulin family, high mobility group box-1 (HMGB-1, also known as amphoterin), CD11b (Mac-1, CD18), amyloid-α peptide, and β-sheet fibrils (see review in Ref. 8).

The extracellular domain of the transmembrane RAGE protein consists of ligand-binding C1, C2, and V domains. The V and C1 domains form an integrated structure, where as C2 domain attaches to the V and C1 domain via a flexible linker. Different ligands bind to the different receptor domains (9). The soluble receptor form, sRAGE, lacks the intracellular domain and is generated either through proteolytic cleavage of RAGE or through alternative RNA splicing in humans (10). The alternate spliced sRAGE form is also designated endogenously secreted RAGE. Classically, sRAGE acts as an endogenous inhibitor of RAGE by binding circulating ligands and inhibiting RAGE-induced cellular signaling, tissue damage, and dysfunction (see review in Ref. 8).

RAGE is involved in several pathological processes including diabetes, Alzheimer's disease, systemic amyloidosis, and tumor growth (see review in Ref. 11). In many human diseases, RAGE and its ligands are upregulated, and the increase in RAGE-induced signaling is a poor prognostic factor for a variety of diseases. For example, AGE and RAGE are upregulated in diabetes and are implicated in complications, including nephropathy (12), retinopathy (13), and cardiovascular complications (14). RAGE is also implicated in atherosclerosis (15). RAGE expression and the interaction between RAGE and HMGB-1 are associated with tumor cell metastasis (16, 17).

Exploiting the anti-inflammatory properties of sRAGE appears to be beneficial for several diseases. Treatment of diabetic mice with sRAGE or neutralizing RAGE Abs restores wound healing and prevents pathological kidney changes by decreasing the expression of matrix metalloproteinases and proinflammatory cytokines TNF-α and IL-6 (see review in Refs. 14, 18, 19). Similarly, the absence of RAGE or administration of sRAGE reduces mortality in animals with septic shock (20). Blocking RAGE signaling using anti-RAGE Abs or sRAGE reduces tumor growth and decreases tumor metastases (see review in Ref. 18). It has been shown that sRAGE could act as a decoy for oxidized low-density lipoprotein during inflammation. The binding of sRAGE to the modified low-density lipoprotein prevents CD36 scavenger receptor-mediated uptake by macrophages and subsequently reduces foam cell formation in atherosclerotic plaques (21). Although these observations support an anti-inflammatory role for sRAGE, sRAGE is also associated with the development of inflammation.

In type II diabetic patients, elevated serum sRAGE levels correlate with inflammation (22). sRAGE is elevated in the serum of septic patients and correlates with severity and mortality (23). Recently, Pullerits and colleagues (24) demonstrated sRAGE induces IL-6 and TNF-α production in splenocytes. Taken together, sRAGE has both pro- and anti-inflammatory properties.

Unlike other tissues in the body, lung tissue expresses high levels of endogenous RAGE and sRAGE (25). This finding may reflect the lung's constant interface with environmental Ags. For example, in lung tissue from patients with idiopathic pulmonary fibrosis, both RAGE and sRAGE are reduced (26). Similarly, RAGE is down-regulated in non-small cell lung

carcinoma (27). Importantly, aged RAGE$^{-/-}$ mice develop fibrotic-like disease in their lungs (25).

To mediate these diverse effects, RAGE activation in monocytes, macrophages, and endothelial and smooth muscle cells triggers the activation of several intracellular pathways, including NF-κB (28), p21ras, MAPKs, and cdc42/rac (16). Neuronal cell survival is mediated by RAGE binding S100 protein, leading to NF-κB activation (29). However, the biological function of RAGE and sRAGE on human primary monocytes and macrophages is elusive.

Based on studies reporting the anti-inflammatory properties of sRAGE, we initially proposed that exogenous sRAGE would act as a decoy molecule to sequester RAGE ligands, limiting monocyte/macrophage activity and lung inflammation. Contrary to our initial hypothesis, we found that exogenous sRAGE directly caused inflammation by recruiting monocytes and neutrophils in vivo and in vitro. In addition, sRAGE directly bound to mononuclear phagocytes to promote monocyte survival and differentiation to macrophages. These processes were modulated through the sRAGE-induced activation of Akt, p38, Erk, and NF-κB and reduced caspase-3 activation in primary human monocytes. Thus, the data presented in this study demonstrate that sRAGE acts as a proinflammatory molecule when administered to the lung. Thus, it is conceivable that the pro- or anti-inflammatory properties of sRAGE may be dictated by the cellular composition of the inflamed tissue, including the availability of ligands in the tissue environment.

Materials and Methods

Reagents

Endotoxin-free RPMI 1640, DPBS, and lymphocyte separation medium were purchased from Mediatec (Herndon, VA). X-VIVO 15 serum-free media was purchased from BioWhittaker (Walkersville, MD). Endotoxin-free FBS (<0.06 EU/ml) was obtained from Atlanta Biological (Lawrenceville, GA). Recombinant sRAGE protein was purified free of detectable endotoxin as described previously (30). Recombinant human M-CSF, GM-CSF, and CCL2 were purchased from R&D Systems (Minneapolis, MN). rG-CSF (Amgen, Thousand Oaks, CA) was purchased through the pharmacy from The Ohio State University Hospital (Columbus, OH).

Fluorescently labeled Abs recognizing CD11b, CD68, CCR5, and mannose receptor (CD206) were obtained from BD Biosciences (San Jose, CA). Chrome pure human or mouse IgG was purchased from Jackson ImmunoResearch Laboratories (West Grove, PA). Abs for Western blot analysis were obtained from Santa Cruz Biotechnology (Santa Cruz, CA) or Cell Signaling Technology (Beverly, MA). U0126 and LY294002 were purchased from EMD Calbiochem (La Jolla, CA). All other reagents were purchased from Sigma-Aldrich (St. Louis, MO) unless indicated otherwise.

sRAGE administration and lung immunohistochemical analysis

Four to 8-wk-old C57BL/6 mice weighing 16–19 g underwent intratracheal (IT) injection with or without 5 μg sRAGE in 100 μl PBS per gram of mouse weight. Positive control mice received 200 μg LPS in PBS, and negative control mice received mouse serum albumin (MSA) in PBS (MSA/PBS). Mice were sacrificed 1 or 2 d postinjection, the whole lungs were harvested, and the tissues were subjected to immunohistochemical analysis or cell isolation. For immunohistochemistry for CD11b expression, the lung was quickly frozen in dry ice with OCT frozen tissue embedding medium (Sakura-Finetek Torrance, CA). Alternatively, the lung tissue was fixed in 10% formalin prior to staining for F4/80. The tissue was paraffin-embedded, cut, and placed on positively charged slides, then baked in a

60° C oven for 1 h. Slides were deparaffinized by rehydration with xylene and graded ethanol solutions. All slides were quenched for 5 min in a 3% hydrogen peroxide solution then blocked with 10% normal rabbit serum and digested with proteinase K for 10 min at 37°C. The slides were stained with CD11b or F4/80 Abs, then detected by Vectastain Elite system with DAB^+ chromogen (Vector Laboratories, Burlingame, CA) and counter-stained with hematoxylin followed with the appropriate secondary Ab. The slides were quantified by histogram analysis using Adobe Photoshop CS (Adobe Systems, Mountain View, CA) as previously described (31). Data are presented as the percent of positive cells per high-power field (HPF) in 10 images and are expressed as the mean ± SEM.

Cell culture conditions and isolation

Human acute monocytic leukemia cell line, THP1 (American Type Culture Collection, Manassas, VA) was maintained in RPMI 1640 (Invitrogen, Carlsbad, CA) supplemented with 10% FBS and 1% antibiotic-antimycotic solution containing penicillin, streptomycin, and amphotericin. Peripheral blood monocytes were isolated from buffy coats obtained from the American Red Cross (Columbus, OH) and purified by positive selection using the CD14 Monocyte Isolation Kit from Miltenyi Biotec (Auburn, CA) as described previously (32). The purity of the monocytes was 97 ± 3% $CD14^+$ as identified by flow cytometry. To obtain monocyte-derived macrophages (MDMs), freshly isolated monocytes were cultured with RPMI 1640 medium supplemented with 10% FBS, 10 μg/ml polymyxin B, and 20 ng/ml M-CSF at 37°C incubator. The length of deriving MDMs was indicated in the figure legends.

Human neutrophils were isolated from whole blood of healthy donors by layering blood/PBS (1:1) over lymphocytes separation medium (Mediatech, Manassas, VA), then the pellet containing RBCs and neutrophils was mixed with dextran sulfate solution (0.9% NaCl and 3% dextran sulfate) and incubated at room temperature for 1 h as previously described (33). The top layer was washed in PBS, and RBCs were lysed in RBC lysis buffer. The purity of the neutrophils was >90% as identified by Wright-Giemsa staining (Thermo Fisher Scientific, Waltham, MA).

To obtain a single-cell suspension from mouse tissue, the mouse lungs or spleens were digested with DNase/collagenase solution (0.5% collagenase type 1, 0.02% DNase I, 1% FBS in RPMI 1640 medium), as described previously with minor modification (34). Briefly, the tissue was cut with a McIlwain Tissue Chopper (Ted Pella, Redding, CA), then digested with DNase/collagenase solution at 37°C for 30 min. The mixture was passed through a 100-μm nylon filter to remove tissue particles. RBCs were then lysed from single-cell suspensions using RBC lysis buffer (0.8% ammonium chloride, 0.1% potassium bicarbonate, 12 mM EDTA). The cells were subjected to flow cytometry analysis.

Mouse monocytes and tissue macrophages were obtained by negative selection using the Mouse Monocytes Enrichment Kit from StemCell Technologies (Vancouver, British Columbia, Canada) following the manufacturer's instructions with minor modification. Briefly, bone marrow was collected from mouse femurs and tibias with a 1-ml insulin syringe. Cells were passed through a 100-μm nylon filter, and RBCs were lysed. Mouse monocytic cells were further purified from the spleens using the Purple EasySep magnet (StemCell Technologies) prior to flow cytometry analysis.

Flow cytometry analysis of extracellular Ags

Human and mouse cells were obtained and resuspended in flow cytometry buffer (1% BSA and 0.1% sodium azide in DPBS). MDMs were removed from tissue culture dishes using accutase (eBioscience, San Diego, CA). Human or mouse IgG was used to block FcγRs followed by extracellular marker staining on ice for 30 min using fluorescently conjugated

Ly6G (clone: 1A8), F4/80 (clone: A3-1), and CD11b (clone: M1/70) Abs. The cells were washed in flow cytometry buffer and fixed in 1% paraformaldehyde solution prior to flow cytometry analysis (FACSCalibur or LSR II, BD Biosciences). Data was analyzed using FCS3 Express software from De Novo Software (Los Angeles, CA). To identify cell subpopulation, data are presented as percentage of positive cells per total number of cells. To quantify surface Ag expression, data are presented as the relative fold increase of the geometric mean over Ab control (AbC) for each day (mean ± SEM).

Monocyte and neutrophil chemotaxis assay

Chemotaxis assays using 48-well modified Boyden chemotaxis chambers (Neuroprobe, Rockville, MD) were described previously for monocytes (35) and neutrophils (36). Briefly, for the monocyte migration assay, sRAGE (5 ng/ml–5 μg/ml) or negative control (PBS) or positive control (10 ng/ml CCL2) was loaded into the bottom chamber. $CD14^+$ monocytes (1×10^6 monocytes/ml) in Gey's Balanced Salt Solution was added to the upper chamber with a 5-μm polyvinylidene difluoride filter specifically designed for monocyte chemotaxis assays (GE Osmonics, Minnetonka, MN). For neutrophil migration assay, 3×10^6 neutrophils/ml was loaded in a Boyden chamber containing a 3-μm polyvinylpyrrolidone-free polycarbonate filter. IL-8 (20 ng/ml) (PeproTech, Rocky Hill, NJ) served as a positive control. The chambers were incubated for 1.5 h at 37°C in a 5% CO_2 incubator. Afterwards, the filters were removed, fixed, and stained in Diff-Quik solution (Thermo Fisher Scientific). Recruited monocytes or neutrophils were quantified by enumerating at least six HPFs using an Olympus 1 × 50 inverted microscope (Olympus, Center Valley, PA). sRAGE-induced chemotaxis is presented as a percent of monocytes or neutrophils recruited by sRAGE over monocytes or neutrophils recruited by their respective positive controls. The data are expressed as means ± SEM. All experiments were performed in triplicate.

Caspase-3 activation

Monocytes (5×10^6 cells/condition) were incubated in X-VIVO 15 medium with sRAGE (0.5–5 μg/ml) or M-CSF (20 ng/ml) overnight at 37°C. The next day, both the floating and adherent cells were washed in ice-cold PBS medium and resuspended in lysis buffer (50 mM HEPES [pH 7.4], 100 mM NaCl, 0.1% CHAPS, 0.1 mM EDTA, and the protease inhibitor 4-[2-aminoethyl] benzenesulfonyl fluoride hydrochloride). The cell pellets were quickly frozen in liquid nitrogen and thawed at room temperature twice. Protein concentration was measured using a BCA protein assay kit (Thermo Fisher Scientific). Lysates were centrifuged at 14,000 × *g* for 10 min at 4°C, and 50 μl cell extract was mixed with 50 μl assay buffer (50 mM HEPES [pH 7.4], 100 mM NaCl, 0.1% CHAPS, 20% glycerol, 10 mM DTT, and 0.1 mM EDTA) and 5 μl of 2 mM fluorogenic substrate Ac-DEVD-AMC (EMD Chemicals, Gibbstown, NJ). The mixture was placed in a single well of a 96-well black clear-bottom plate (Corning Glass, Corning, NY) and immediately subjected to kinetic fluorometric assay using a Cytofluor 4000 fluorometer (Perseptive, Framingham, MA) with filters of 360 nm excitation and 460 nm emission for up to 2 h. The linear change of the fluorescence of hydrolyzed free AMC was used to calculate caspase-3 activity. Caspase-3 activity is presented as the relative fold increase in sRAGE-stimulated sample readout over GM-CSF–stimulated sample readout per total protein and is expressed as the mean ± SEM.

Annexin V-FITC/propidium iodide apoptosis assay

$CD14^+$ monocytes (5×10^6 cells/condition) were incubated in X-VIVO 15 medium with sRAGE (0.5–5 μg/ml) or M-CSF (20 ng/ml) overnight at 37°C. Then, both suspension and adherent cells were stained with an Annexin V-FITC apoptosis detection kit (BD Pharmingen, San Diego, CA) as described previously (32). Percent of Annexin V-FITC–positive cells were used to identify apoptotic cells. Data are presented as the relative fold

increase of percent of Annexin V-FITC–positive cells from sRAGE-treated cells over M-CSF–treated and are expressed as the mean ± SEM.

Human monocyte transfection and NF-κB activity assay

Transient transfection of primary human monocytes was performed using the Amaxa Nucleofector system (Lonza Walkersville, Walkersville, MD) as described previously (32). The NF-κB–luc reporter assay was performed as described previously (37). Briefly, monocytes (15×10^6 cells) isolated from buffy coats were resuspended in Monocyte Transfection Solution (Lonza) containing 2 μg NF-κB–Luc construct and transfected using the Amaxa program Y-01. The cells were immediately washed in warm X-VIVO 15 medium and plated in 3 wells of a 12-well plate. The monocytes were incubated with or without 5 μg/ml sRAGE in a 37°C incubator for 24 h, and luciferase production was measured with the Luciferase Assay System using a Luminometer (Promega, Madison, WI). Data are presented as the relative fold increase of mock transfected over nonstimulated (NS) sample and are expressed as the mean ± SEM.

Cytokine production

$CD14^+$ monocytes (5×10^6 cells/condition) were incubated in X-VIVO 15 medium containing sRAGE (5 μg/ml), MSA control, or M-CSF (100 ng/ml) for 24–48 h at 37°C. The supernatants were collected and assayed for inflammatory cytokine production using Bio-Rad Bioplex System (Bio-Rad, Hercules, CA) according to the manufacturer's protocol.

Western blot analysis

Prior to stimulation, $CD14^+$ monocytes (10×10^6 cells/condition) were plated for 1 h, then stimulated with sRAGE (0–10 μg/ml), M-CSF (20 ng/ml), or GM-CSF (25 ng/ml). For MDM studies, cells were serum starved for 2 h prestimulation. For kinetic analysis, we ensured that all cells were in culture for the same length of the time. For NF-κB nuclear translocation experiments, cytosolic and nuclear fractions were separated using a Sigma Cell-lytic Nuclear extraction kit (Sigma-Aldrich). For whole-cell lysate, cells were lyzed on ice for 15 min in 1× lysis buffer (Cell Signaling Technology) containing protease inhibitor mixture III (EMD Calbiochem). Lysates were cleared of insoluble material, and the protein concentration was determined using Bio-Rad Protein Assay (Bio-Rad). The samples were separated by SDS-PAGE, transferred to a nitrocellulose membrane, probed with the indicated Abs, and detected by ECL (Amersham Biosciences, Piscataway, NJ). The ECL signal was quantified using the Quantity One densitometry program (Bio-Rad). Protein expression and phosphorylation protein was normalized to either β-actin or total protein, respectively. Data are expressed as fold change of NS samples over stimulated samples.

Binding of sRAGE to cell surface

Recombinant sRAGE, G-CSF, and GM-CSF were labeled using an Alexa Fluor 488 mAb Labeling Kit (Invitrogen) following the manufacturer's instructions with minor modification. Briefly, 100 μg protein was resuspended in PBS containing 0.1 M sodium bicarbonate buffer and incubated with Alexa Fluor 488 for 1 h at room temperature with gentle mixing every 15 min following overnight incubation at 4°C. Labeled protein was purified by passing through a size exclusion spin column, and 2 mg/ml BSA was added to stabilize the labeled protein. Approximately 50% recombinant protein was recovered postlabeling.

Monocytes or MDMs were incubated with human IgG for 15 min, incubated with 2.5 μg/ml labeled protein on ice for 1 h, washed with flow cytometry wash buffer, and fixed in 1% paraformaldehyde solution before flow cytometry analysis.

For competition assays, M-CSF–derived MDMs were removed using accutase, then incubated with human IgG for 15 min, then incubated with different concentrations of unlabeled sRAGE (0–10 μg/ml) on ice for 1 h, and washed before incubating with 2.5 μg/ml labeled sRAGE on ice for 1 h. The cells were washed with flow cytometry wash buffer and fixed in 1% paraformaldehyde solution before flow cytometry analysis.

Statistical analysis

All data are expressed as the mean ± SEM derived from at least three independent studies. The number of independent times each experiment was repeated is indicated in the figure legends. Statistical analysis for immunohistochemical staining and flow cytometry analysis was performed with SPSS16 software (SPSS, Chicago, IL) by using independent sample *t* tests. Flow cytometry studies were analyzed with Wilcoxon signed-rank *t* test. ANOVA was used to compare treatment effects on caspase-3 and NF-κB activity, and one-sample *t* test was applied for the Western blot analysis. Holm's method was used to adjust for multiplicity and control the overall type I error rate at $\alpha = 0.05$. These analyses were completed using SAS software (version 9.1, SAS Institute, Cary, NC). Statistical significance was defined as $p \leq 0.05$.

Results

sRAGE induces macrophage infiltration in the murine lung in vivo

RAGE is highly expressed in the lung and primarily in the alveolar epithelium, where it has been identified as a basolateral marker protein for type I lung alveolar cells (38). In addition, RAGE expression is abundant in mononuclear phagocytes and can modulate both pro- and anti-inflammatory responses (see review in Ref. 7). Because alveolar macrophages are important in maintaining lung homeostasis, we wanted to understand whether sRAGE injected directly into murine lungs affected immune homeostasis. We injected recombinant sRAGE IT into C57BL/6 mice. IT injection of LPS served as a positive control. After 24 or 48 h post-injection, lungs were harvested, and cellular recruitment was identified by either immunohistochemical analysis or flow cytometry. Immunohistochemistry staining (Fig. 1*A*–*D*) revealed increased expression of both CD11b and F4/80 markers in lung tissue from animals treated with sRAGE- compared with PBS-injected mice ($p < 0.01$). Because both neutrophils and monocytes express CD11b and neutrophils are increased in lavage fluid following i.p. administration of sRAGE (24), we further analyzed the cell populations in the lungs after sRAGE injection. Therefore, single-cell suspensions from the lungs were subjected to flow cytometric staining to identify neutrophils ($LY6G^+/F480^-$) and macrophages ($CD11b^+/LY6G^-$) (39, 40). Both neutrophils ($LY6G^+F4/80^-$) (Fig. 1*E*) and monocytes/macrophages ($LY6G^-CD11b^+$) (Fig. 1*F*) were increased in the lungs of mice that were injected IT with sRAGE versus those injected with PBS/MSA. Notably, sRAGE recruited fewer neutrophils than LPS (Fig. 1*E*). In contrast, sRAGE recruited more monocytes/macrophages than LPS at 24 h, but not at 48 h postinjection (Fig. 1*F*).

sRAGE recruits human monocytes and neutrophils in vitro

Because IT sRAGE injection led to monocyte and neutrophil accumulation in vivo, we next examined whether sRAGE directly induced human monocyteor neutrophil recruitment invitro. Primary human monocytes or neutrophils were isolated and chemotaxis assays were performed using sRAGE (5 ng/ml–5 μg/ml), PBS/MSA vehicle (negative control), or CCL2 (10 ng/ml) as a positive control for monocyte chemotaxis. IL-8 served as a positive control for neutrophil chemotaxis. Shown in Table I, sRAGE-stimulated peripheral human monocyte recruitment was 3.5–6.0-fold higher than PBS/MSA ($p < 0.05$ for all dosages of sRAGE), whereas sRAGE significantly recruited human neutrophils at a rate 1.6–2.0-fold higher than PBS/MSA ($p < 0.01$).

sRAGE induces proinflammatory cytokine production in human monocytes

sRAGE can induce the production of the proinflammatory cytokines IL-6 and TNF-α and the chemokine CCL3/MIP-1α (24). Given that sRAGE recruited human monocytes and neutrophils in vitro, we examined whether sRAGE modulated the production of chemokines and/or proinflammatory cytokines. Compared to PBS/MSA-treated cells, sRAGE-treated monocytes produced greater amounts of the proinflammatory cytokines IL-1β and IL-6 and chemokines CCL3 and CCL4 (Table II; $p < 0.001$). However, CCL5 and platelet-derived growth factor (PDGF)-bb was not increased in cells treated with sRAGE compared with PBS/MSA stimulation.

We also confirmed the cell purity of the isolated monocytes by flow cytometry using surface Ags to identify monocytes (CD14), T cells (CD3), B cells (CD19), and neutrophils (CD66b) in sRAGE-treated cells. Using these markers, the isolated cells were at least 97% pure monocytes (data not shown). These observations indicate that the cytokine production was most likely from monocytes in response to sRAGE.

sRAGE mediates human peripheral monocyte differentiation into macrophages

Because sRAGE led to monocyte and macrophage accumulation in the lungs of treated mice, we next tested whether sRAGE modulated the differentiation of human monocytes into macrophages in vitro. Primary human monocytes were treated with human rM-CSF (20 ng/ml) or GM-CSF (25 ng/ml) (positive controls), PBS (negative control), or sRAGE (0.25–10 μg/ml) in serum-free X-VIVO medium overnight. Cells were visualized using phase-contrast microscopy (Fig. 2). As expected, M-CSF– and GM-CSF–treated human monocytes assumed the characteristic phenotypic changes of differentiated macrophages by assuming elongated and irregular shapes and becoming adherent. Interestingly, sRAGE-treated monocytes phenotypically mimicked cells treated with M-CSF or GM-CSF. Moreover, the phenotypic responses in monocytes were dose dependent, and sRAGE concentrations as low as 0.5 μg/ml induced some phenotypic changes in human monocytes (data not shown). Because 5 μg/ml sRAGE was found to optimally induce the phenotypic changes, all subsequent experiments were performed using this concentration.

As an additional control, we confirmed that macrophage maturation was not due to the presence of contaminating endotoxin. Because the endotoxin level of recombinant sRAGE was 65.2 ± 1.5 pg/ml, a parallel set of samples was treated with this LPS concentration in the presence of polymyxin B without sRAGE. We failed to detect macrophage differentiation in these cells (data not shown). Taken together, sRAGE treatment stimulated monocyte differentiation into macrophages.

We next confirmed that the cellular phenotypic changes corresponded to changes in surface Ag expression indicative of macrophage differentiation (Fig. 3). Macrophages express mannose receptors (CD206), but resting monocytes do not (41). CCR5 is a chemokine receptor and expressed predominantly on macrophages, T cells, and dendritic cells, and the expression of CCR5 increases during monocyte differentiation (42). Therefore, we measured the expression of the mannose receptor and CCR5 on the cell surface. Compared to cells stained with isogenic AbC, surface mannose receptor expression increased over time for both sRAGE and M-CSF–treated cells ($p = 0.01$ on day 3 and $p = 0.043$ on day 5) (Fig. 3*A*, 3*B*). Similarly, CCR5 expression increased in sRAGE-treated monocytes and in M-CSF–treated cells (Fig. 3*C*, 3*D*). Furthermore, we found that MHC class II expression was increased upon sRAGE stimulation in human monocytes, suggesting sRAGE-derived macrophages are functionally active and have the ability to present Ag (data not shown).

Promotion of monocyte survival by sRAGE through decreased caspase-3 activity and increased NF-κB activity

Modulation of cell survival through NF-κB activation is an important step in cellular differentiation. Substantial evidence shows that RAGE/AGE ligation induces NF-κB activity and genes linked to inflammation (for review see Ref. 8). Therefore, we next assessed whether sRAGE modulated cell survival and NF-κB activity in human monocytes. We previously showed that inflammatory cytokines and growth factors promote monocyte survival by suppressing caspase-3 activity (1, 43). Therefore, we first explored the effect of sRAGE on cell survival by measuring caspase-3 activity after overnight stimulation with or without sRAGE. As shown in Fig. 4*A*, in the absence of growth factor stimulation (NS), human monocytes underwent apoptosis and displayed a 6.72 ± 1.89-fold increase in caspase-3 activity compared with M-CSF–stimulated cells (positive control). Compared with NS cells, sRAGE treatment significantly suppressed caspase-3 activity in human monocytes ($p < 0.05$ at sRAGE concentration of 0.5 μg/ml and 1 μg/ml and $p < 0.01$ at sRAGE concentration of 5 μg/ml). Notably, 5 μg/ml sRAGE appeared to be equally effective as M-CSF (100 ng/ml) at suppressing caspase-3 activity.

As an alternative method of measuring cell apoptosis, we measured annexin V/propidium iodide (PI) staining in treated cells by flow cytometry. Apoptotic cells are Annexin V^+/PI^-(early apoptosis) and Annexin V^+/PI^+ populations (late apoptosis). In this study, we combined percent of Annexin V^+/PI^- cells and percent of Annexin V^+/PI^+ cells as apoptotic cells. Compared to M-CSF–treated cells, sRAGE protected monocytes from apoptosis in a dose-dependent manner (Fig. 4*B*). Monocytes exposed to sRAGE stimulation had reduced apoptotic cells compared with the NS monocytes at concentrations of 1–10 μg/ml. Collectively, these data showed that sRAGE promoted human monocyte survival.

Because NF-κB activation by growth factors correlates to monocyte survival (37), we examined whether sRAGE activated NF-κB in monocytes. To measure NF-κB activity, monocytes were transiently transfected with an NF-κB–Luc cDNA construct encoding luciferase. Following overnight stimulation with sRAGE, the presence of luciferase was measured. As shown in Fig. 4*C*, sRAGE treatment induced a significant increase in luciferase production in human monocytes compared with PBS-treated cells (NS) ($p = 0.015$). Activation of NF-κB is associated with release from the cytoplasmic inhibitor IκB and translocation of NF-κB into the nucleus to bind the promoter region of NF-κB–regulated genes. We therefore examined the nuclear translocation of NF-κB in the treated cells. As shown in Fig. 4*D*, the majority of p65 was located in the cytosol when cells were quiescent, but nuclear translocation occurred upon sRAGE stimulation. To evaluate cross-contamination between the nuclear and cytosolic preparations, the membranes were also immunoblotted using Abs recognizing LaminB and GAPDH. As expected, Lamin B was present exclusively in the nuclear fraction, whereas GAPDH was detected in the cytosol fraction. Quantification of the Western blot data by band densitometry confirmed that there was a 2.7–3.3-fold increase of nuclear translocation of NF-κB in sRAGE-stimulated samples over NS samples (Fig. 4*E*). Taken together, these observations demonstrate that sRAGE induces NF-κB transcriptional activity in human monocytes.

Intracellular signaling activated by sRAGE in human monocytes and MDMs

Previous studies demonstrated that binding of RAGE by ligand triggers activation of different cellular signaling pathways, such as GTPases (Cdc42, Rac) (17), p38 MAPK, and stress-activated protein kinase/JNK (16). We previously reported that Akt, Erk, and p38 activation are important in monocyte survival (5, 32); thus, we next examined whether sRAGE induced these signaling pathways in monocytes. As shown in Fig. 5, phosphorylation of Erk and Akt was apparent in sRAGE-treated monocytes. Using a linear

regression analysis to examine sRAGE-induced Akt and Erk phosphorylation over time, we found that phosphorylation of both proteins were significantly increased ($p < 0.001$ and $p = 0.001$, respectively) and maximal Erk and Akt activation was observed 2 and 3 h poststimulation, respectively (Fig. 5*A*, 5*C*). In contrast, MDMs responded more rapidly to sRAGE. As shown in Fig. 5*B* and 5*D*, phosphorylation of Akt and Erk were significantly enhanced following stimulation with sRAGE. Akt phosphorylation was maximal at 1 h, whereas Erk phosphorylation was maximal at 30 min ($p = 0.033$ and $p = 0.024$ compared with PBS-stimulated cells, respectively). We also found p38 MAPK and JNK phosphorylation occurred after sRAGE stimulation in MDMs; sRAGE activated p38 MAPK and JNK activity within 2 h and 30 min of treatment, respectively (data not shown). Because sRAGE activated Akt and Erk more rapidly in macrophages compared with monocytes, our data indicated that macrophages might be more amenable to activation by sRAGE.

sRAGE-induced monocyte survival and differentiation is inhibited by PI3K inhibitors and MEK inhibitors

Because Akt and Erk activation are important for macrophage cell survival and differentiation (2), we next examined whether inhibition of these pathways reduced sRAGE-mediated survival and/or differentiation. Therefore, we pretreated the cells with the MEK inhibitor U0126 (10 μM), the PI-3K inhibitor LY294002 (50 μM), or solvent DMSO for 1 h at 37°C prior to sRAGE stimulation for 2 or 3 h, which corresponded to the maximal Erk and Akt activation, respectively. As shown in Fig. 6*A*, LY294002 reduced Akt phosphorylation induced by sRAGE, and U0126 specifically reduced Erk phosphorylation induced by sRAGE at both time points. Importantly, both LY294002 and U0126 inhibited sRAGE-stimulated cell survival as indicated by enhanced caspase-3 activity ($p = 0.012$ sRAGE-treated plus inhibitors versus sRAGE-treated plus DMSO samples) (Fig. 6*B*). Furthermore, both LY294002 ($p = 0.046$ compared with sRAGE-treated samples) and U0126 ($p = 0.028$ compared with treated samples) prevented sRAGE-activated expression of mannose receptor in viable cells (Fig. 6*C*). As a control, we performed trypan blue exclusion analysis and found that the inhibitors used did not cause nonspecific cell toxicity (data not shown). These observations indicate that PI3K and MAPK pathways are activated by sRAGE to modulate monocyte survival and differentiation.

sRAGE binds the cell surface of monocytes and MDMs

The majority of studies report sRAGE acts as a decoy receptor that competes for ligand with RAGE (see review in Ref. 8). Because sRAGE can activate cellular signaling, we hypothesized that sRAGE bound directly to the cell surface. Using Alexa Fluor 488 fluorescently labeled sRAGE protein, we found that sRAGE bound to the surface of both monocytes and macrophages as measured by flow cytometry (Fig. 7*A*, 7*B*). Monocytes incubated with Alexa Fluor 488-labeled sRAGE exhibited a 1.43-fold increase in geometric mean over Alexa Fluor 488 AbC ($p < 0.05$) (Fig. 7*C*). In comparison with monocytes, we found a 2.65-fold increase in sRAGE binding to the cell surface of MDMs compared with cells incubated with control Abs ($p = 0.012$) (Fig. 7*C*). Furthermore, we examined the kinetics of sRAGE binding to the cell surface over time and found that the binding of sRAGE to the cell surface correlated with monocyte maturation (Fig. 7*D*). Because both monocytes and macrophages express GM-CSFRs (see review in Refs. 44, 45), we used labeled GM-CSF as a positive control for our studies. Labeled GM-CSF bound to monocytes and MDMs equally well over the time-course experiment ($p = 0.045$ compared with FITC-labeled isogenic Abs (Fig. 7*D*). Because G-CSFR is highly expressed on human monocytes (46) and declines during macrophage differentiation (47), we also examined expression of G-CSFR as an additional control. As expected, we observed that labeled human G-CSF bound to monocytes ($p = 0.045$), but did not bind to MDMs ($p = 0.43$).

Because sRAGE seems to have a higher binding affinity toward MDMs, we performed competitive binding assay using unlabeled sRAGE. We found a significant dose-dependent decrease in the surface binding of labeled sRAGE in the presence of unlabeled sRAGE (Fig. 7*E*, 7*F*). Compared to cells incubated without unlabeled sRAGE (100%), a reduction in sRAGE binding by 79% or 61% was apparent in cells incubated with either 5 μg/ml (2-fold excess) or 10 μg/ml (4-fold excess) of unlabeled sRAGE, respectively (Fig. 7*F*; $*p < 0.05$ versus Alexa 488-labeled sRAGE). In general, these data provided evidence that sRAGE directly binds to the cell surface of monocytes and macrophages.

Because sRAGE preferentially bound to the surface of MDMs compared with monocytes, we examined whether the binding characteristics of sRAGE were similar on freshly isolated immature monocytes and mature tissue macrophages. As shown in Fig. 7*G*, tissue macrophages isolated from the spleen had a higher affinity for sRAGE than bone marrow monocytes.

sRAGE binds to a premonocytic cell line, THP1, but fails to activate downstream events that lead to differentiation

Because sRAGE directly bound to monocytes and induced their differentiation, we were interested in understanding whether sRAGE also mediated myeloid differentiation of THP1 leukemic cells. To test our hypothesis, we first examined whether sRAGE bound to the cell surface of the myelomonocytic cell line THP1. We found a 1.3-fold increase in surface binding of labeled sRAGE on THP1 cells compared with FITC-labeled isogenic AbC ($p = 0.043$) (Fig. 8*A*, 8*B*). Importantly, THP1 cells treated with sRAGE failed to differentiate as measured by cellular adherence, even after 4 d of incubation with sRAGE (Fig. 8*C*), or activate Erk signaling (Fig. 8*D*, 8*E*). As a positive control, THP1 cells were treated with PMA to induce cellular differentiation, which resulted in Erk phosphor-ylation and cellular adherence (Fig. 8*C–E*). This observation indicated that the binding of sRAGE to the cell surface was not sufficient to induce differentiation. Thus, taken together, binding of sRAGE to the cell surface is necessary, but not sufficient, to induce differentiation, whereas cellular adherence correlates with cell differentiation in the presence of sRAGE

Adherence of monocytes appears important for sRAGE-induced cellular differentiation

The adherence of monocytes facilitates their differentiation, prolongs cell survival, and primes these cells to respond to external stimuli (48). To examine the role of cellular adherence in sRAGE-induced signaling and differentiation, we compared Akt and Erk activation as well as differentiation in monocytes incubated with sRAGE in tubes or on tissue-culture plates (Fig. 9*A–C*). We observed that Akt and Erk phosphorylation were significantly higher in sRAGE-stimulated cells cultured on plates than in tubes (Fig. 9*A–C*; $p < 0.05$ for cells plated versus cultured in suspension). Furthermore, cells incubated with sRAGE on plates had higher surface expression of mannose receptors than cells cultured with sRAGE in tubes ($p = 0.046$; Fig. 9*D*, 9*E*). Interestingly, the benefit of adherence was conserved if other maturation signals like M-CSF were used instead of sRAGE ($p = 0.028$ for cells plated versus cultured in suspension) (Fig. 9*D*, 9*E*). Therefore, cellular adherence appeared to be an important costimulus for sRAGE-induced differentiation of human monocytes. To ensure that adherence did not directly affect sRAGE binding to cells, we collected the cells at day 1 and found that cells bound sRAGE equally when cultured in tubes or on plates (data not shown). Therefore, these observations confirm that binding of sRAGE to the cell surface is necessary, but not sufficient, to induce differentiation.

sRAGE-induced monocyte differentiation and binding to the cell surface are not dependent on β_2 integrin (Mac-1/CD11b) binding

To define binding sites of sRAGE on human monocytes and MDMs, we hypothesized that sRAGE complexed with other surface receptors to transduce signaling events. An attractive target is Mac1/CD11b (24). We incubated monocytes with CD11b blocking or isogenic Abs (clone M1/70; BD Pharmingen) before stimulating with sRAGE. In contrast to our hypothesis, we failed to observe any significant difference in monocyte differentiation, caspase-3 activity, or cell surface binding of sRAGE between cells treated with either CD11b plus sRAGE and IgG2b plus sRAGE (Supplemental Fig. 1). The Arg-Gly-Asp (RGD) peptide is known to block cellular recognition sites for numerous adhesion proteins including integrins present in the extracellular matrix and in blood (49). We also incubated RGD peptide and its scrambled control peptide before stimulating with sRAGE and again found no difference between RGD plus sRAGE and scramble plus sRAGE (Supplemental Fig. 1). This indicated that sRAGE binding to the cell surface and sRAGE-induced macrophage differentiation were not solely dependent on β_2 integrin (Mac-1/CD11b) binding.

Discussion

RAGE functions as a pattern recognition receptor for a number of proteins, including AGEs (50). sRAGE has been reported to be a competitive inhibitor of RAGE-mediated cellular activation events by sequestering its ligands (see review in Ref. 8). Recent studies indicate that sRAGE has both anti- and proinflammatory properties. To test the properties of the sRAGE within the lung, we IT injected sRAGE into mouse lungs and found sRAGE induced inflammation. Our result showed that sRAGE led to the migration and accumulation of monocytes and neutrophils into the lungs in vivo and induced monocyte and neutrophil recruitment in vitro. sRAGE also induced the survival and differentiation of human blood monocytes by stimulating downstream Akt, Erk, and NF-κB activity. Notably, sRAGE bound directly to cell surfaces of monocytes and MDMs and appeared to preferentially bind to mature cells. Cellular adherence also appeared to be an important costimulus for cellular survival and differentiation by sRAGE. Therefore, in addition to cellular recruitment, our studies demonstrate that sRAGE induced monocyte survival and differentiation in vitro indicating a novel role for sRAGE in host inflammation.

Previously, we identified the activation of Akt, Erk, and NF-κB as critical factors in human monocyte survival (5, 51). It is interesting that sRAGE activated these signaling pathways and reduces caspase-3 activation in the absence of growth factor stimulation. Of note, several studies demonstrate that inhibiting RAGE function leads to cell proliferation and survival. Bartling et al. (27) found that RAGE blockade using anti-RAGE Abs or sRAGE induces fibroblast cell proliferation and Erk activation. Similarly, using specific siRNAs to knock down RAGE expression increases proliferation of A549 epithelial cells and fibroblasts (26). In addition, overexpression of full-length RAGE leads to death of the lung cancer cell line, H358 (27). Aleshin et al. (52) found hearts from $RAGE^{-/-}$ mice have significantly less caspase-3 activation and TUNEL-positive nuclei versus wild-type heart after ischemic challenge, suggesting blocking RAGE function increases cardiomyocyte survival. Therefore, we wondered if sRAGE promoted monocyte survival and differentiation was simply from blocking RAGE function. To address this question, we treated human monocytes with sRAGE in vitro and found that sRAGE bound directly to the cells and stimulated their migration, survival, and differentiation. These data show ed that sRAGE directly induced monocyte activation.

In this study, we also demonstrated that sRAGE leads to enhanced production of proinflammatory cytokines and chemokines in human monocytes. Our in vitro chemotaxis

assay further showed that sRAGE has the ability to induce migration of both monocytes and neutrophils. A previous report showed that the β_2-microglobulin modified form of AGE induced monocyte migration and prevented apoptosis. sRAGE could inhibit AGE–β_2-microglobulin cellular recruitment (53); however, the investigators did not examine the effect of sRAGE alone on monocyte chemotaxis as we report in this study. Consistent with our finding, sRAGE induced neutrophil chemotaxis in mice (24).

To elucidate the mechanisms by which sRAGE activated monocytes, we examined whether sRAGE directly interacted with the surface of human monocytes. We found that sRAGE bound directly to the surface of human monocytes and MDMs. Interestingly, MDMs had a greater affinity for sRAGE binding than did freshly isolated monocytes. Consistent with this observation, we also found that mature tissue macrophages have a greater affinity for sRAGE than did immature monocytes. These data suggest that cell maturity influenced sRAGE binding. We currently are examining the receptor to which sRAGE binds. Because it is possible that sRAGE is a pattern-recognition ligand, it is likely that sRAGE uses several cell-surface receptors.

Bartling et al. (27) reported that in lung cancer cells, extracellular RAGE preferentially localizes at intercellular contact sites, independent of expression of the cytoplasmic domain, implying RAGE-dependent effects might be mediated exclusively by the extracellular region. In another study, sulfoglucuronyl carbohydrates on neural cells bind amphoterin (secreted HMGB-1), which then interacts with RAGE on an adjacent cell to facilitate cellular communication (54). It is possible that sRAGE binds to the surface of target cells to facilitate cell–cell interactions and activate downstream signaling events.

To define binding sites of sRAGE on human monocytes and MDMs, we tested whether sRAGE complexed with surface receptors to transduce signaling events. It has been reported that sRAGE can interact with Mac1/CD11b (24). However, we failed to observe any significant difference in monocyte differentiation, caspase-3 activity, or sRAGE binding to the cell surface between anti-CD11b plus sRAGE- and IgG2b plus sRAGE-treated cells. We further found that blocking cellular sites used by adhesion molecules with the RGD peptide did not effectively inhibit sRAGE binding or cellular activation. Further studies are needed to clarify sRAGE binding partners in promoting monocyte survival and differentiation.

We also attempted to investigate whether sRAGE bound negative regulatory factors that inhibit monocyte survival and differentiation as the mechanism of action. However, our evidence did not support this as the mechanism of action, given the direct in vitro effects of sRAGE. Depleting sRAGE from conditioned monocyte supernatant did not affect monocyte survival or differentiation (data not shown), suggesting that sRAGE likely acted by directly binding to the cell surface and inducing intracellular signaling. Lastly, we also examined the possibility that growth factors known to induce monocyte survival and differentiation (like M-CSF and GM-CSF) were induced by sRAGE stimulation or that M-CSF or GM-CSF induced sRAGE to mediate these effects. However, we failed to detect sRAGE secretion from monocytes treated with either M-CSF or GM-CSF by ELISA or M-CSF or GM-CSF production in sRAGE-treated monocyte supernatants (data not shown).

In our study, we also found that sRAGE bound the surface of immature premyelocytic cells but did not activate the cells. We observed that freshly isolated monocytes bound sRAGE to activate intracellular signaling pathways including Akt and Erk in adherent cells. In contrast, sRAGE failed to activate Akt and Erk phosphorylation in THP1 cells. Because THP1 are transformed leukemic cells, it is possible that these observations reflect a failure of sRAGE to overcome the intrinsic defects in maturation. We also found that adherence was an

important costimulatory factor for sRAGE in nonadherent monocytes, even though sRAGE bound to cells in suspension.

Taking our data presented in this study in context with published literature, we propose two roles for sRAGE in regulating monocyte and macrophage cellular activation: 1) sRAGE works as a RAGE decoy to reduce inflammation in certain types of cells by binding RAGE ligands, thus reducing their interaction with surface RAGE (see review in Ref. 8); and 2) when ligands are not in excess, sRAGE can mediate inflammation by directly binding to leukocytes to subsequently induce migration, survival, and differentiation of these cells.

In summary, our findings indicate a novel property of sRAGE in vivo that mediates monocyte and neutrophil inflammation in murine lungs and directly promotes their recruitment, as well as monocyte survival and differentiation. sRAGE treatment of adherent mononuclear phagocytes led to the activation of Akt and MAPK kinase pathways and increased NF-κB activity. Because sRAGE has diverse functions in regulating inflammation, it is possible that sRAGE plays an important role in macrophage maturation. Further understanding the function of sRAGE will likely provide therapeutic approaches for treatment of RAGE-dependent inflammatory events.

Acknowledgments

We thank Christie Newland and Shannon Wells at the animal core facility of the Center for Critical Care, The Ohio State University Medical Center, for assistance in animal studies. We also thank Gary Phillips at the Center for Biostatistics, The Ohio State University, for statistical consultation, Mark Julian for performing endotoxin analysis of sRAGE, and Dr. Timothy Eubank for advice on figure preparation.

This work was supported by Grant R01 HL067176 from the National Heart, Lung, and Blood Institute (to C.B.M.). M.G.P. is a Parker B. Francis Fellow in Pulmonary Research. H.W. is a visiting scholar from Qingdao Municipal Hospital (People's Republic of China).

Abbreviations used in this paper

AbC	Ab control
AGE	advanced glycation end products
HMGB-1	high mobility group box-1
HPF	high-power field
IT	intra-tracheal
MDM	monocyte-derived macrophage
MSA	mouse serum albumin
NS	nonstimulated
PDGF	platelet-derived growth factor
PI	propidium iodide
RAGE	receptor for advanced glycation end products
RGD	Arg-Gly-Asp
sRAGE	soluble form of the receptor for advanced glycation end products

References

1. Goyal A, Wang Y, Graham MM, Doseff AI, Bhatt NY, Marsh CB. Monocyte survival factors induce Akt activation and suppress caspase-3. Am J Respir Cell Mol Biol. 2002; 26:224–230. [PubMed: 11804874]
2. Hunter M, Wang Y, Eubank T, Baran C, Nana-Sinkam P, Marsh C. Survival of monocytes and macrophages and their role in health and disease. Front Biosci. 2009; 14:4079–4102. [PubMed: 19273336]
3. Chitu V, Stanley ER. Colony-stimulating factor-1 in immunity and inflammation. Curr Opin Immunol. 2006; 18:39–48. [PubMed: 16337366]
4. Lutz MB. IL-3 in dendritic cell development and function: a comparison with GM-CSF and IL-4. Immunobiology. 2004; 209:79–87. [PubMed: 15481143]
5. Bhatt NY, Kelley TW, Khramtsov VV, Wang Y, Lam GK, Clanton TL, Marsh CB. Macrophage-colony-stimulating factor-induced activation of extracellular-regulated kinase involves phosphatidylinositol 3-kinase and reactive oxygen species in human monocytes. J Immunol. 2002; 169:6427–6434. [PubMed: 12444151]
6. Neeper M, Schmidt AM, Brett J, Yan SD, Wang F, Pan YC, Elliston K, Stern D, Shaw A. Cloning and expression of a cell surface receptor for advanced glycosylation end products of proteins. J Biol Chem. 1992; 267:14998–15004. [PubMed: 1378843]
7. Schmidt AM, Hori O, Cao R, Yan SD, Brett J, Wautier JL, Ogawa S, Kuwabara K, Matsumoto M, Stern D. RAGE: a novel cellular receptor for advanced glycation end products. Diabetes. 1996; 45(Suppl 3):S77–S80. [PubMed: 8674899]
8. Herold K, Moser B, Chen Y, Zeng S, Yan SF, Ramasamy R, Emond J, Clynes R, Schmidt AM. Receptor for advanced glycation end products (RAGE) in a dash to the rescue: inflammatory signals gone awry in the primal response to stress. J Leukoc Biol. 2007; 82:204–212. [PubMed: 17513693]
9. Dattilo BM, Fritz G, Leclerc E, Kooi CW, Heizmann CW, Chazin WJ. The extracellular region of the receptor for advanced glycation end products is composed of two independent structural units. Biochemistry. 2007; 46:6957–6970. [PubMed: 17508727]
10. Schlueter C, Hauke S, Flohr AM, Rogalla P, Bullerdiek J. Tissue-specific expression patterns of the RAGE receptor and its soluble forms—a result of regulated alternative splicing? Biochim Biophys Acta. 2003; 1630:1–6. [PubMed: 14580673]
11. Yan SD, Schmidt AM, Stern D. Alzheimer's disease: inside, outside, upside down. Biochem Soc Symp. 2001; 67:15–22. [PubMed: 11447831]
12. Wendt TM, Tanji N, Guo J, Kislinger TR, Qu W, Lu Y, Bucciarelli LG, Rong LL, Moser B, Markowitz GS, et al. RAGE drives the development of glomerulosclerosis and implicates podocyte activation in the pathogenesis of diabetic nephropathy. Am J Pathol. 2003; 162:1123–1137. [PubMed: 12651605]
13. Yamamoto Y, Kato I, Doi T, Yonekura H, Ohashi S, Takeuchi M, Watanabe T, Yamagishi S, Sakurai S, Takasawa S, et al. Development and prevention of advanced diabetic nephropathy in RAGE-overexpressing mice. J Clin Invest. 2001; 108:261–268. [PubMed: 11457879]
14. Yan SF, Yan SD, Herold K, Ramsamy R, Schmidt AM. Receptor for advanced glycation end products and the cardiovascular complications of diabetes and beyond: lessons from AGEing. Endocrinol Metab Clin North Am. 2006; 35:511–524. viii. [PubMed: 16959583]
15. Ramasamy R, Yan SF, Herold K, Clynes R, Schmidt AM. Receptor for advanced glycation end products: fundamental roles in the inflammatory response: winding the way to the pathogenesis of endothelial dysfunction and atherosclerosis. Ann NY Acad Sci. 2008; 1126:7–13. [PubMed: 18448789]
16. Taguchi A, Blood DC, del Toro G, Canet A, Lee DC, Qu W, Tanji N, Lu Y, Lalla E, Fu C, et al. Blockade of RAGE-amphoterin signalling suppresses tumour growth and metastases. Nature. 2000; 405:354–360. [PubMed: 10830965]
17. Huttunen HJ, Fages C, Rauvala H. Receptor for advanced glycation end products (RAGE)-mediated neurite outgrowth and activation of NF-kappaB require the cytoplasmic domain of the receptor but different downstream signaling pathways. J Biol Chem. 1999; 274:19919–19924. [PubMed: 10391939]

18. Schmidt AM, Yan SD, Yan SF, Stern DM. The multiligand receptor RAGE as a progression factor amplifying immune and inflammatory responses. J Clin Invest. 2001; 108:949–955. [PubMed: 11581294]
19. Logsdon CD, Fuentes MK, Huang EH, Arumugam T. RAGE and RAGE ligands in cancer. Curr Mol Med. 2007; 7:777–789. [PubMed: 18331236]
20. Liliensiek B, Weigand MA, Bierhaus A, Nicklas W, Kasper M, Hofer S, Plachky J, Gröne HJ, Kurschus FC, Schmidt AM, et al. Receptor for advanced glycation end products (RAGE) regulates sepsis but not the adaptive immune response. J Clin Invest. 2004; 113:1641–1650. [PubMed: 15173891]
21. Marsche G, Weigle B, Sattler W, Malle E. Soluble RAGE blocks scavenger receptor CD36-mediated uptake of hypochlorite-modified low-density lipoprotein. FASEB J. 2007; 21:3075–3082. [PubMed: 17536039]
22. Nakamura K, Yamagishi S, Adachi H, Kurita-Nakamura Y, Matsui T, Yoshida T, Imaizumi T. Serum levels of sRAGE, the soluble form of receptor for advanced glycation end products, are associated with inflammatory markers in patients with type 2 diabetes. Mol Med. 2007; 13:185–189. [PubMed: 17592553]
23. Bopp C, Hofer S, Weitz J, Bierhaus A, Nawroth PP, Martin E, Büchler MW, Weigand MA. sRAGE is elevated in septic patients and associated with patients outcome. J Surg Res. 2008; 147:79–83. [PubMed: 17981300]
24. Pullerits R, Brisslert M, Jonsson IM, Tarkowski A. Soluble receptor for advanced glycation end products triggers a proinflammatory cytokine cascade via beta2 integrin Mac-1. Arthritis Rheum. 2006; 54:3898–3907. [PubMed: 17133598]
25. Englert JM, Hanford LE, Kaminski N, Tobolewski JM, Tan RJ, Fattman CL, Ramsgaard L, Richards TJ, Loutaev I, Nawroth PP, et al. A role for the receptor for advanced glycation end products in idiopathic pulmonary fibrosis. Am J Pathol. 2008; 172:583–591. [PubMed: 18245812]
26. Queisser MA, Kouri FM, Königshoff M, Wygrecka M, Schubert U, Eickelberg O, Preissner KT. Loss of RAGE in pulmonary fibrosis: molecular relations to functional changes in pulmonary cell types. Am J Respir Cell Mol Biol. 2008; 39:337–345. [PubMed: 18421017]
27. Bartling B, Hofmann HS, Weigle B, Silber RE, Simm A. Down-regulation of the receptor for advanced glycation end-products (RAGE) supports non-small cell lung carcinoma. Carcinogenesis. 2005; 26:293–301. [PubMed: 15539404]
28. Alves M V, Calegari C, Cunha DA, Saad MJ, Velloso LA, Rocha EM. Increased expression of advanced glycation end-products and their receptor, and activation of nuclear factor kappa-B in lacrimal glands of diabetic rats. Diabetologia. 2005; 48:2675–2681. [PubMed: 16283249]
29. Huttunen HJ, Kuja-Panula J, Sorci G, Agneletti AL, Donato R, Rauvala H. Coregulation of neurite outgrowth and cell survival by amphoterin and S100 proteins through receptor for advanced glycation end products (RAGE) activation. J Biol Chem. 2000; 275:40096–40105. [PubMed: 11007787]
30. Park L, Raman KG, Lee KJ, Lu Y, Ferran LJ Jr, Chow WS, Stern D, Schmidt AM. Suppression of accelerated diabetic atherosclerosis by the soluble receptor for advanced glycation endproducts. Nat Med. 1998; 4:1025–1031. [PubMed: 9734395]
31. Lehr HA, Mankoff DA, Corwin D, Santeusanio G, Gown AM. Application of photoshop-based image analysis to quantification of hormone receptor expression in breast cancer. J Histochem Cytochem. 1997; 45:1559–1565. [PubMed: 9358857]
32. Wang Y, Zeigler MM, Lam GK, Hunter MG, Eubank TD, Khramtsov VV, Tridandapani S, Sen CK, Marsh CB. The role of the NADPH oxidase complex, p38 MAPK, and Akt in regulating human monocyte/macrophage survival. Am J Respir Cell Mol Biol. 2007; 36:68–77. [PubMed: 16931806]
33. Piper MG, Massullo PR, Loveland M, Druhan LJ, Kindwall-Keller TL, Ai J, Copelan A, Avalos BR. Neutrophil elastase downmodulates native G-CSFR expression and granulocyte-macrophage colony formation. J Inflamm (Lond). 2010; 7:5. [PubMed: 20205821]
34. Swanson KA, Zheng Y, Heidler KM, Mizobuchi T, Wilkes DS. CDllc+ cells modulate pulmonary immune responses by production of indole-amine 2,3-dioxygenase. Am J Respir Cell Mol Biol. 2004; 30:311–318. [PubMed: 12959949]

35. Ali NA, Gaughan AA, Orosz CG, Baran CP, McMaken S, Wang Y, Eubank TD, Hunter M, Lichtenberger FJ, Flavahan NA, Lawler J, Marsh CB. Latency associated peptide has in vitro and in vivo immune effects independent of TGF-beta1. PLoS ONE. 2008; 3:e1914. [PubMed: 18392110]
36. Frevert CW V, Wong A, Goodman RB, Goodwin R, Martin TR. Rapid fluorescence-based measurement of neutrophil migration in vitro. J Immunol Methods. 1998; 213:41–52. [PubMed: 9671124]
37. Wang Y, Keogh RJ, Hunter MG, Mitchell CA, Frey RS, Javaid K, Malik AB, Schurmans S, Tridandapani S, Marsh CB. SHIP2 is recruited to the cell membrane upon macrophage colony-stimulating factor (M-CSF) stimulation and regulates M-CSF-induced signaling. J Immunol. 2004; 173:6820–6830. [PubMed: 15557176]
38. Shirasawa M, Fujiwara N, Hirabayashi S, Ohno H, Iida J, Makita K, Hata Y. Receptor for advanced glycation end-products is a marker of type I lung alveolar cells. Genes Cells. 2004; 9:165–174. [PubMed: 15009093]
39. Tsou CL, Peters W, Si Y, Slaymaker S, Aslanian AM, Weisberg SP, Mack M, Charo IF. Critical roles for CCR2 and MCP-3 in monocyte mobilization from bone marrow and recruitment to inflammatory sites. J Clin Invest. 2007; 117:902–909. [PubMed: 17364026]
40. Tacke F, Randolph GJ. Migratory fate and differentiation of blood monocyte subsets. Immunobiology. 2006; 211:609–618. [PubMed: 16920499]
41. Pontow SE, Kery V, Stahl PD. Mannose receptor. Int Rev Cytol. 1992; 137B:221–244. [PubMed: 1478821]
42. Tuttle DL, Harrison JK, Anders C, Sleasman JW, Goodenow MM. Expression of CCR5 increases during monocyte differentiation and directly mediates macrophage susceptibility to infection by human immunodeficiency virus type 1. J Virol. 1998; 72:4962–4969. [PubMed: 9573265]
43. Zeigler MM, Doseff AI, Galloway MF, Opalek JM, Nowicki PT, Zweier JL, Sen CK, Marsh CB. Presentation of nitric oxide regulates monocyte survival through effects on caspase-9 and caspase-3 activation. J Biol Chem. 2003; 278:12894–12902. [PubMed: 12566444]
44. Suzu S, Motoyoshi K. Signal transduction in macrophages: negative regulation for macrophage colony-stimulating factor receptor signaling. Int J Hematol. 2002; 76:1–5. [PubMed: 12138890]
45. Suzuki H, Katayama N, Ikuta Y, Mukai K, Fujieda A, Mitani H, Araki H, Miyashita H, Hoshino N, Nishikawa H, et al. Activities of granulocyte-macrophage colony-stimulating factor and interleukin-3 on monocytes. Am J Hematol. 2004; 75:179–189. [PubMed: 15054806]
46. Boneberg EM, Hareng L, Gantner F, Wendel A, Hartung T. Human monocytes express functional receptors for granulocyte colony-stimulating factor that mediate suppression of monokines and interferon-gamma. Blood. 2000; 95:270–276. [PubMed: 10607712]
47. Barreda DR, Hanington PC, Belosevic M. Regulation of myeloid development and function by colony stimulating factors. Dev Comp Immunol. 2004; 28:509–554. [PubMed: 15062647]
48. Bauer GJ, Arbabi S, Garcia IA, de Hingh I, Rosengart MR, Maier RV. Adherence regulates macrophage signal transduction and primes tumor necrosis factor production. Shock. 2000; 14:435–440. [PubMed: 11049106]
49. Maheshwari G, Brown G, Lauffenburger DA, Wells A, Griffith LG. Cell adhesion and motility depend on nanoscale RGD clustering. J Cell Sci. 2000; 113:1677–1686. [PubMed: 10769199]
50. Yan SF, Ramasamy R, Naka Y, Schmidt AM. Glycation, inflammation, and RAGE: a scaffold for the macrovascular complications of diabetes and beyond. Circ Res. 2003; 93:1159–1169. [PubMed: 14670831]
51. Kelley TW, Graham MM, Doseff AI, Pomerantz RW, Lau SM, Ostrowski MC, Franke TF, Marsh CB. Macrophagecolony-stimulating factorpromotes cell survival through Akt/protein kinaseB. J Biol Chem. 1999; 274:26393–26398. [PubMed: 10473597]
52. Aleshin A, Ananthakrishnan R, Li Q, Rosario R, Lu Y, Qu W, Song F, Bakr S, Szabolcs M, D'Agati V, et al. RAGE modulates myocardial injury consequent to LAD infarction via impact on JNK and STAT signaling in a murine model. Am J Physiol Heart Circ Physiol. 2008; 294:H1823–H1832. [PubMed: 18245563]
53. Miyata T, Hori O, Zhang J, Yan SD, Ferran L, Iida Y, Schmidt AM. The receptor for advanced glycation end products (RAGE) is a central mediator of the interaction of AGE-

beta2microglobulin with human mononuclear phagocytes via an oxidant-sensitive pathway. Implications for the pathogenesis of dialysis-related amyloidosis. J Clin Invest. 1996; 98:1088–1094. [PubMed: 8787669]

54. Chou DK, Zhang J, Smith FI, McCaffery P, Jungalwala FB. Developmental expression of receptor for advanced glycation end products (RAGE), amphoterin and sulfoglucuronyl (HNK-1) carbohydrate in mouse cerebellum and their role in neurite outgrowth and cell migration. J Neurochem. 2004; 90:1389–1401. [PubMed: 15341523]

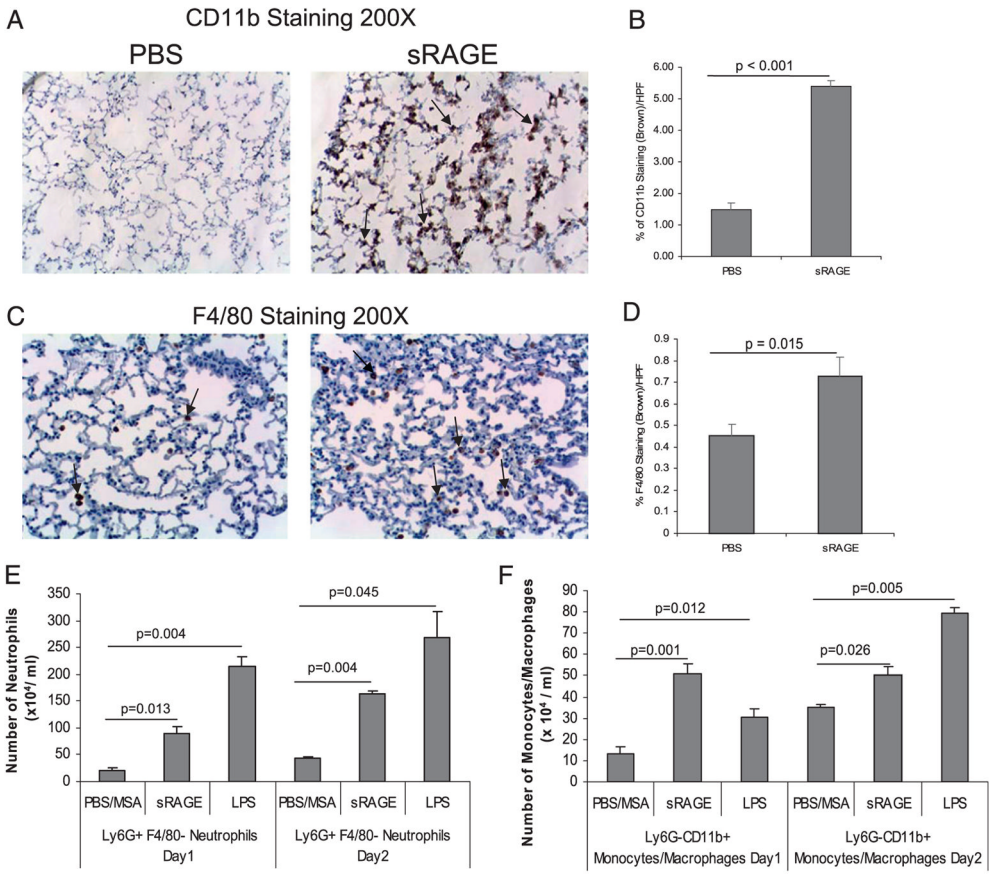

FIGURE 1.

sRAGE induces macrophage and neutrophil infiltration in the murine lung in vivo. C57/BL6 mice were injected IT with 5.0 μg sRAGE per gram of mouse weight, 200 μg LPS, or 200 μg PBS/MSA for 1 or 2 d. Lungs were harvested and subjected to immunohistochemical staining for CD11b (*A*) or F4/80 (*C*) expression. Ten pictures per slide were taken using an Olympus 1 × 50 inverted microscope equipped with a 20× objective and Nikon camera (Olympus). Brown staining represents $CD11b^+$ cells (*A*) or $F4/80^+$ cells (*C*). The images were quantified by histogram analysis using Adobe Photoshop CS (*B*, *D*). Shown are representative pictures obtained from three pairs of mice. Single-cell suspension from the lungs were also stained with Ly6G, F4/80, and CD11b Abs and analyzed by flow cytometry. Neutrophils were defined as $Ly6G^+$ $F4/80^-$ population (*E*), and monocytic cells were defined as Ly6G–$CD11b^+$ population (*F*). Data presented are the percent positive cells from the total cell number obtained from at least three different mice and are expressed as the mean ± SEM.

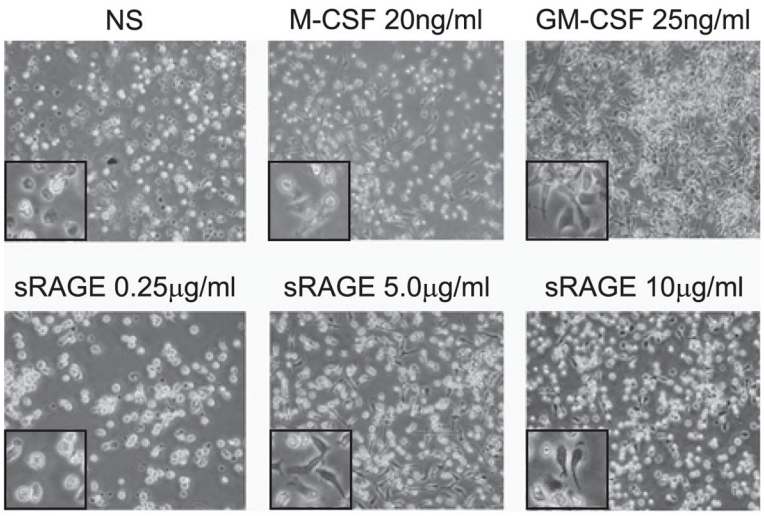

FIGURE 2.

Induction of phenotypic changes in human peripheral monocytes by sRAGE. $CD14^+$ monocyte (5×10^6) cells were cultured in a six-well plate with X-VIVO 15 medium supplemented with 10 μg/ml polymyxin B sRAGE (0.25–10 μg/ml) in a 37°C incubator. Cells cultured with either M-CSF or GM-CSF served as positive controls. Pictures were taken after 1 d in culture using an Olympus inverted microscope (Olympus) (original magnification × 100). The inset in each picture is an enlarged section of the original image. Shown are representative pictures obtained from six independent donors performed in duplicate.

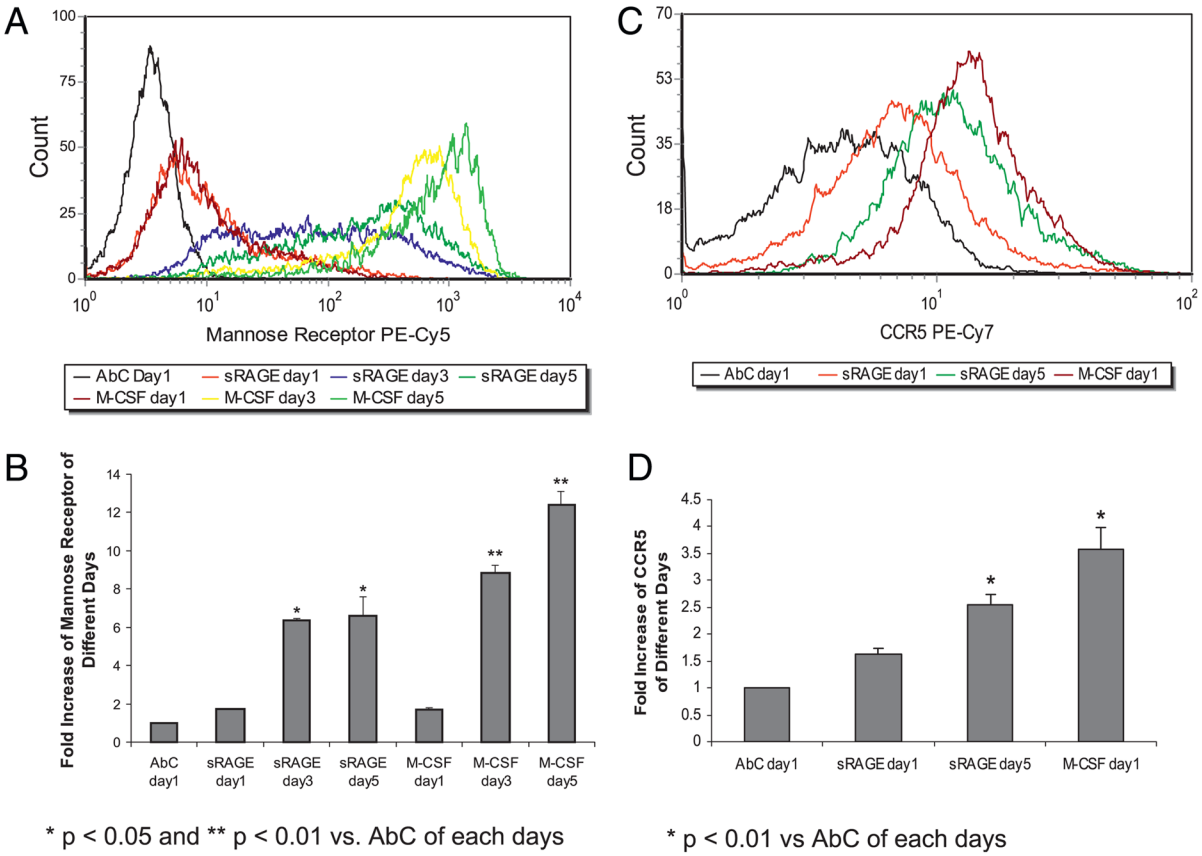

FIGURE 3.

Enhanced surface Ags expression indicative of differentiation on human peripheral monocytes by sRAGE. $CD14^+$ monocytes (5×10^6 cells) were cultured in media with or without 5 μg/ml sRAGE or 100 ng/ml M-CSF. At the indicated times, cells were removed from the plate using accutase and the expression of mannose receptor (*A*, *B*) (*$p < 0.05$; **$p < 0.01$ versus AbC of each day) or CCR5 (*C*, *D*) (*$p < 0.01$ versus AbC of each day) were analyzed by flow cytometry. Data are expressed as the fold increase in geometric mean ± SEM compared with AbC from each time point. Shown are data from three independent donors.

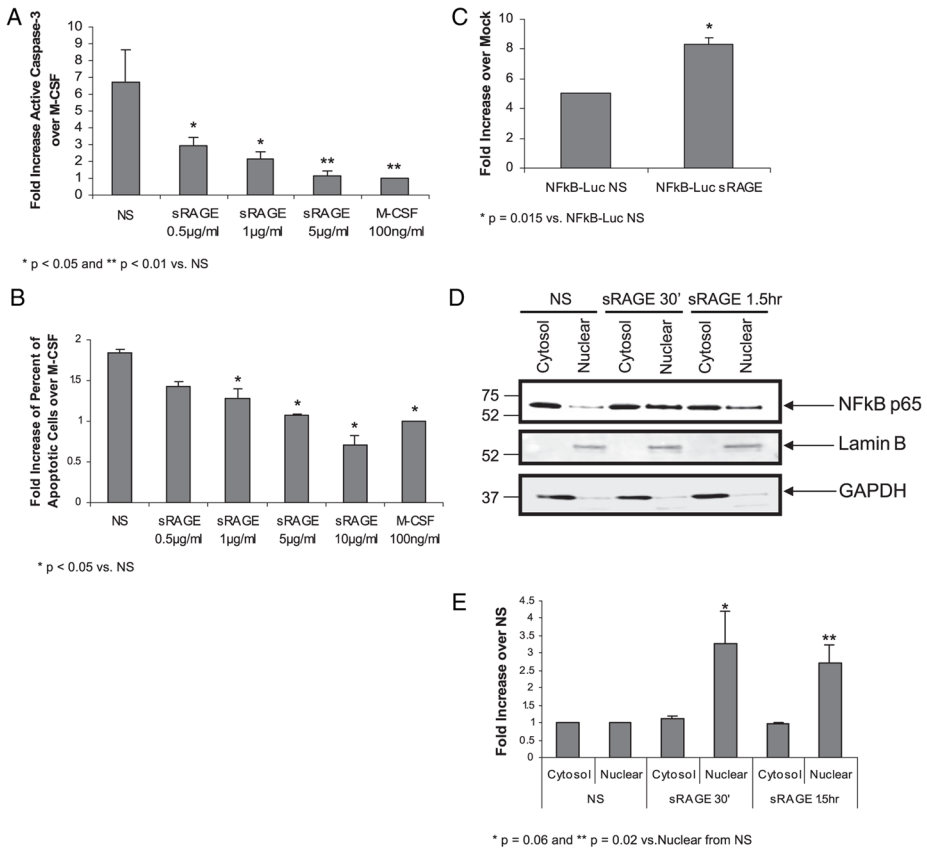

FIGURE 4.

sRAGE promotes cell survival and NF-κB nuclear translocation in human monocytes. Monocytes (5×10^6 cells/well) were cultured in the absence or presence of sRAGE as indicated. *A*, After overnight incubation, cell lysates were assayed for caspase-3 activity using a fluorogenic substrate Ac-DEVD-AMC as described in the *Materials and Methods*. Caspase-3 activity is presented as fold increase in fluorescence of sRAGE-stimulated samples over M-CSF–stimulated samples per total protein. Data are expressed as the mean ± SEM. *$p < 0.05$; **$p < 0.01$ compared with NS samples. *B*, Cells were removed from the plate by accutase and stained with Annexin V/PI for analysis by flow cytometry. Data are presented as fold increase for Annexin V expression of sRAGE-treated cells over M-CSF–treated cells. Shown is the mean ± SEM. *$p < 0.05$ compared with NS samples. *C*, Monocytes (15×10^6 cells/condition) were transfected with 2 μg NF-κB–Luc construct or enhanced GFP control construct then cultured with or without 5 μg/ml sRAGE for 24 h. Luciferase activity was measured with the Luciferase Assay System. Data are presented as the mean relative fold increase ± SEM in luciferase activity comparing transfected cells to mock transfected cells: *$p = 0.015$. Data shown are from three independent donors and assayed in triplicate. *D*, M-CSF–derived MDMs were serum starved overnight and stimulated with 5 μg/ml sRAGE for the indicated times. Equal nuclear and cytosol proteins were analyzed by immunoblotting with p65 NF-κB Ab. The blot was stripped and reblotted with Lamin B or GAPDH Ab to ensure the purity of the nuclear and cytosol fractions. Shown is a representative blot from four independent donors. *E*, Protein expression was quantified by band densitometry, and cytosolic and nuclear fractions were normalized to GAPDH and Lamin B, respectively. Comparison of sRAGE-treated cells to NS cells was performed. *$p = 0.06$; **$p = 0.02$ of nuclear translocation of NF-κB at 30 min and 1 h, respectively.

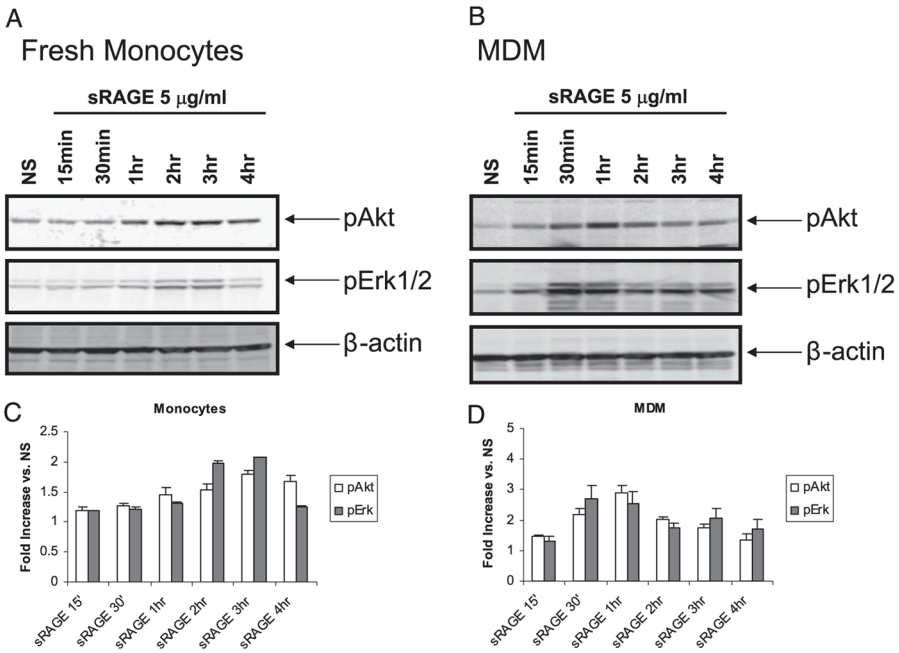

FIGURE 5.

Activation of downstream signaling in human monocytes and monocytes derived macrophages by sRAGE. Protein lysates were generated and immunoblotted for phosphorylation of Akt and Erk from monocytes (*A*) or MDMs (*B*) stimulated with 5 μg/ml sRAGE for indicated times. Equal loading was confirmed by β-actin Ab. Shown are representative data from monocytes or macrophages obtained from three independent donors. Phosphorylation levels were quantified by comparing band densitometry of the *upper panels* and normalizing these values to the β-actin signals in the respective lanes for monocytes (*C*) and MDMs (*D*). Shown is the average fold increase ± SEM over NS controls from three independent donors.

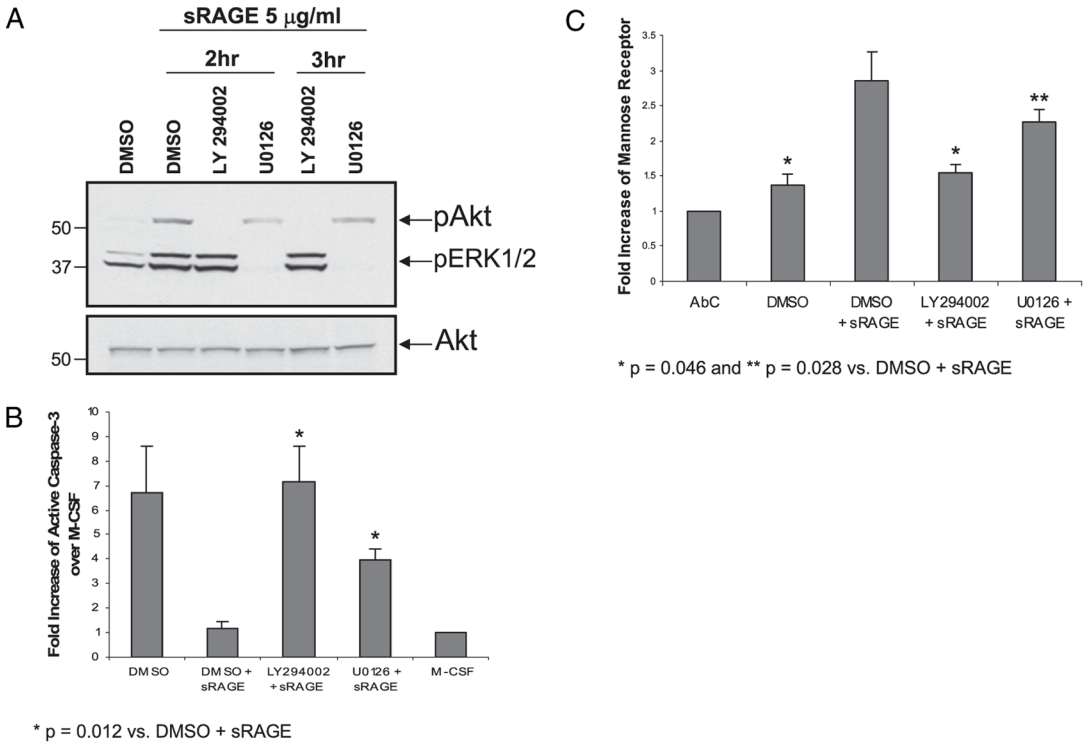

FIGURE 6.

sRAGE modulates cell survival and differentiation through PI3K and Erk intracellular signaling. *A*, Prior to sRAGE stimulation, monocytes were treated with MEK inhibitor U0126 (10 μM), PI3K inhibitor LY294002 (50 μM), or solvent DMSO for 1 h. At the indicated times, cells were lysed, and protein lysates were immunoblotted for phosphorylation of Akt and Erk. Equal loading was confirmed using Akt Ab. Shown is a representative blot from three independent donors. *B*, Monocytes treated in the presence or absence of inhibitors for 1 h were cultured overnight with 100 μg/ml M-CSF or 5 μg/ml sRAGE, then assayed for caspase-3 activity. Data are presented as the mean fold increase ± SEM of caspase-3 activity over M-CSF–treated cells per total protein from six independent donors. $p = 0.012$ compared with DMSO plus sRAGE. *C*, After 2 d in culture with either M-CSF or sRAGE, cells were analyzed for mannose receptor expression by flow cytometry. The data are expressed as the fold increase of geometric mean ± SEM of AbC from macrophages of six independent donors. *$p = 0.046$; **$p = 0.028$ compared with DMSO plus sRAGE.

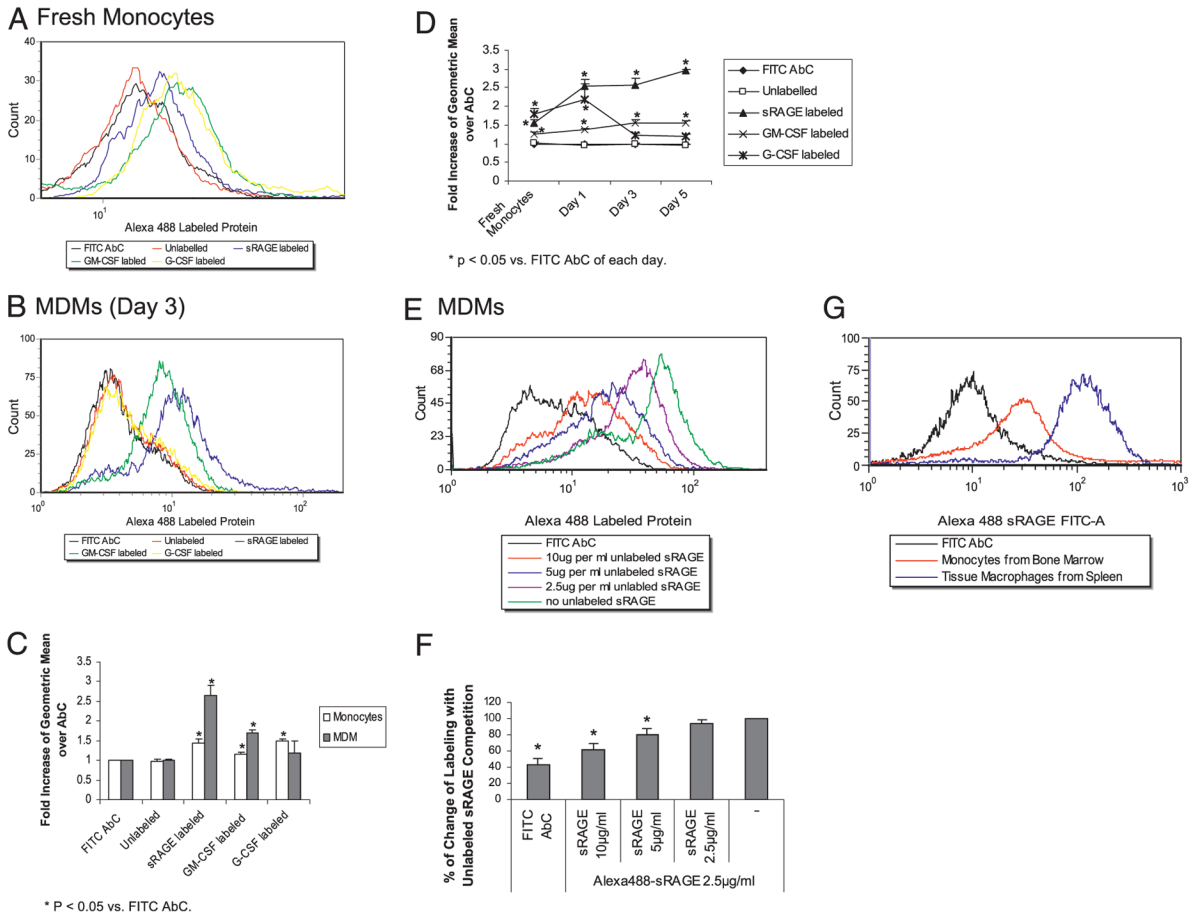

FIGURE 7.

sRAGE binds directly to the cell surface of monocytes and macrophages. Monocytes (5×10^6 cells/ml) (*A*) or MDMs (*B*) were incubated with human IgG for 15 min and then incubated with 2.5 μg/ml Alexa Fluor 488-labeled sRAGE protein on ice for 1 h, washed with flow wash buffer, and fixed in 1% paraformaldehyde solution before flow cytometry analysis. *C*, The flow cytometry data from *A* and *B* are expressed as fold increase of geometric mean ± SEM compared with FITC AbC from four independent donors: $*p < 0.05$ compared with AbC of each day. *D*, Comparison of flow cytometry data over time was performed. The data are expressed as the fold increase of geometric mean ± SEM compared with Alexa Fluor 488 AbC from four independent donors: $*p < 0.05$ compared with AbC of each day. *E*, MDMs were incubated with different concentrations of unlabeled sRAGE on ice for 1 h prior to the incubation with 2.5 μg/ml labeled sRAGE. The cells were analyzed by flow cytometry. *F*, The flow cytometry data from *E* are expressed as percent change of labeling compared with cells without competition. Mean fluorescence intensity of cells incubated without unlabeled sRAGE was used as 100% labeling. The data are expressed as the percent change of geometric mean ± SEM from three independent donors: $*p < 0.05$ versus Alexa Fluor 488-sRAGE. *G*, Monocytes or macrophages were isolated from mouse bone marrow and spleen, respectively. The cells were incubated with mouse IgG for 15 min and then incubated with 2.5 μg/ml Alexa Fluor 488-labeled sRAGE protein on ice for 1 h and fixed in 1% paraformaldehyde solution before flow cytometry analysis. Shown is a representative histogram from two independent mice.

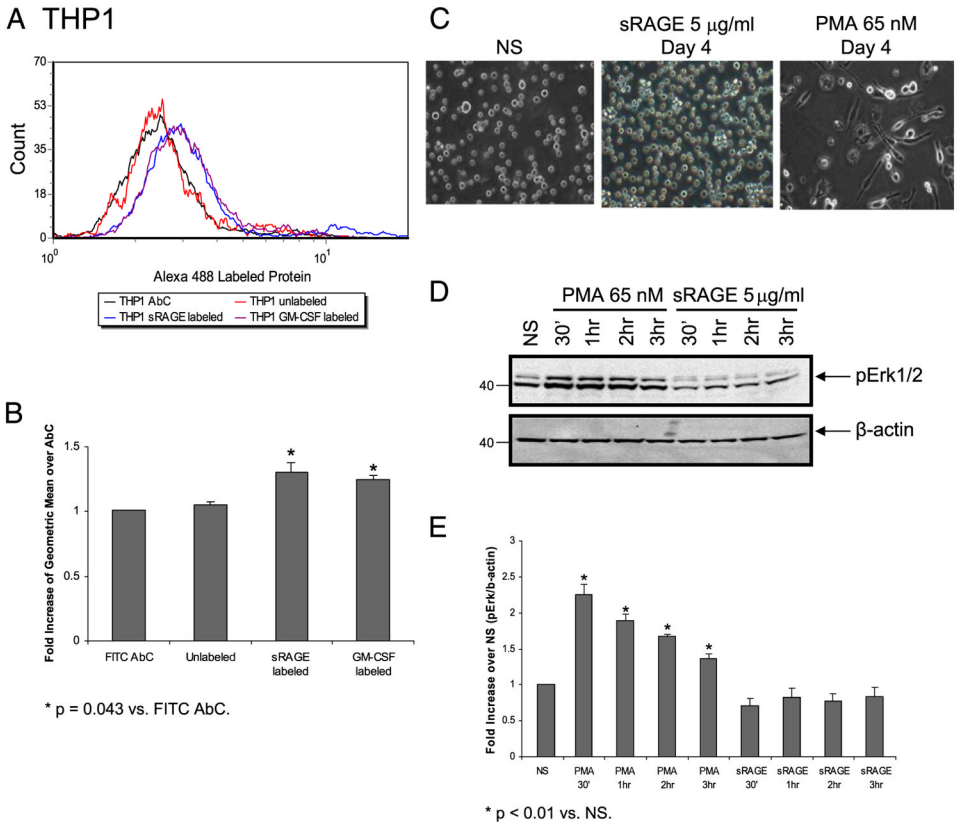

FIGURE 8.

Binding of sRAGE to the cell surface of THP1 cells does not mediate downstream signaling events or differentiation. *A*, THP1 cells (5×10^5) were incubated with human IgG for 15 min, then incubated with 2.5 μg/ml labeled protein on ice for 1 h, and washed with flow wash buffer then subjected to flow cytometry analysis. *B*, Data are expressed as the fold increase of geometric mean ± SEM over FITC AbC from three independent experiments. *p = 0.043 compared with FITC AbC. *C*, THP1 cells (5×10^5) were cultured without (NS) or with 5 μg/ml sRAGE or 65 nM PMA in a 37°C incubator. Photographs were taken daily. Shown are images of cells in cultured for 4 d. *D*, Serum-starved THP1 cells were stimulated with either 65 nM PMA or 5 μg/ml sRAGE or left unstimulated (NS) for indicated times at 37°C. Equal amount of protein was examined for Erk phosphorylation by Western blot analysis. Densitometry of *D* is shown in *E* as fold increase of phospho-Erk over total β-actin from three independent experiments: *$p < 0.01$ compared with NS samples.

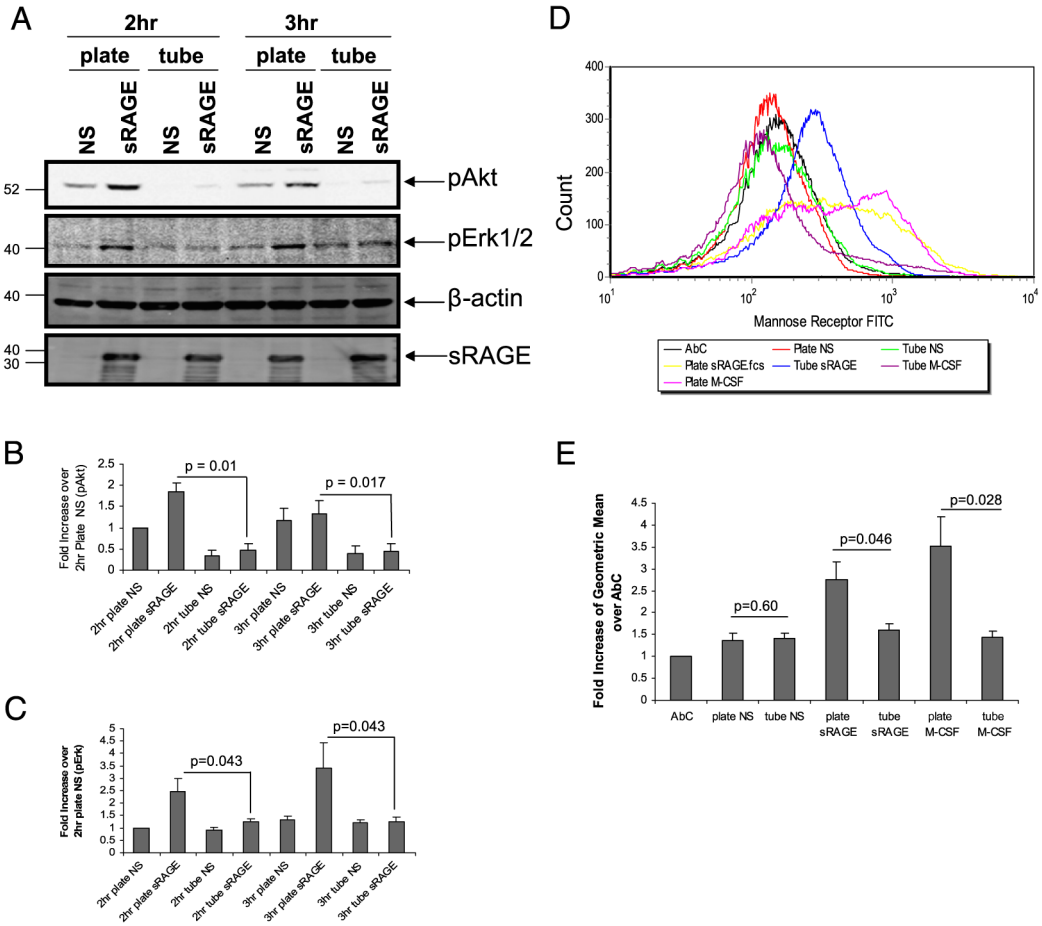

FIGURE 9.

Adherence of monocytes is essential for sRAGE to activate downstream events in human monocytes. Monocytes were stimulated without or with sRAGE (5 μg/ml) in either six-well plates or tubes at 37°C for the indicated times. *A*, Equal amount of protein was analyzed by immunoblotting for phospho-Akt and phospho-Erk. Equal loading was confirmed by β-actin Ab. Phosphorylation levels of Akt (*B*) and Erk (*C*) were quantified by densitometry and normalized to β-actin. *D*, After 2 d in culture, cells were collected and stained for mannose receptor expression by flow cytometry. Shown are representative data from six independent donors. *E*, Data are expressed as the fold increase of geometric mean ± SEM over AbC.

Table I

sRAGE recruited human monocyte and neutrophil chemotaxis

	PBS/MSA	sRAGE (5 ng/ml)	sRAGE (50 ng/ml)	sRAGE (500 ng/ml)	sRAGE (5 μg/ml)	CCL2 (10 ng/ml)	IL-8 (20 ng/ml)
Monocyte	8.59 ± 3.07	53.49 ± 9.16 *	48.78 ± 8.67 *	42.97 ± 11.71 *	32.06 ± 8.85 *	115.16 ± 16.96 **	NA
Neutrophil	25.60 ± 1.63	52.82 ± 3.46 **	42.40 ± 1.49 **	40.54 ± 1.91 **	27.20 ± 1.39	NA	100.00 ± 4.82 **

$CD14^+$ monocytes were isolated from buffy coats, neutrophils were isolated from fresh blood, and 1×10^6 monocytes/ml or 3×10^6 neutrophils/ml were resuspended in Gey's Balanced Salt Solution and assayed for sRAGE-induced chemotaxis using the indicated concentrations. Monocyte or neutrophil quantification was performed by counting at least six HPFs of fixed and stained filters. All experiments were performed in triplicate. Data presented are percent of monocytes or neutrophils recruited by each sRAGE condition or PBS over percent of monocytes recruited by CCL2 or percent of neutrophils recruited by IL8. Shown is the mean ± SEM obtained from four independent donors for monocyte and two independent donors for neutrophil.

* $p < 0.05$ versus PBS-treated control;

** $p < 0.01$ versus PBS-treated control.

Table II

sRAGE enhanced proinflammatory cytokines and chemokines production (pg/ml)

	IL-6	IL-1β	CCL3/MIP-1α	CCL4/MIP-1β	CCL5/RANTES	PDGF-bb
PBS/MSA	3.135 ± 1.07	0.24 ± 0.12	4.83 ± 0.20	162.96 ± 2.07	956.39 ± 121.41	1321.69 ± 50.05
sRAGE (5 μg/ml)	7807.52 ± 80.17	5038.225 ± 356.79	174.55 ± 10.50	5633.11 ± 337.15	1179.43 ± 148.91	1286.39 ± 7.43

$CD14^+$ monocytes (5×10^6 cells/condition) were treated with either PBS/MSA or sRAGE (5 μg/ml). The 24-h supernatant was collected to measure IL-6, IL-1β, CCL3, and CCL4 cytokine production, and the 48-h supernatant was collected to measure CCL5 and PDGF secretion. Cytokines production (pg/ml) was measured by Bio-Rad Bioplex System (Bio-Rad). All experiments were performed in triplicate. Data presented are the mean ± SEM from two independent donors.